# Coupling vector and pseudoscalar mesons to study baryon resonances

K. P. Khemchandani,[1,*] A. Martínez Torres,[2,†] H. Kaneko,[1,‡] H. Nagahiro,[1,3,§] and A. Hosaka[1,‖]

[1]*Research Center for Nuclear Physics (RCNP), Mihogaoka 10-1, Ibaraki 567-0047, Japan*
[2]*Yukawa Institute for Theoretical Physics, Kyoto University, Kyoto 606-8502, Japan*
[3]*Department of Physics, Nara Women's University, Nara 630-8506, Japan*

(Received 11 July 2011; revised manuscript received 13 October 2011; published 15 November 2011)

A study of meson-baryon systems with total strangeness $-1$ is made within a framework based on the chiral and hidden local symmetries. These systems consist of octet baryons, pseudoscalar and vector mesons. The pseudoscalar meson-baryon (PB) dynamics has been earlier found determinant for the existence of some strangeness $-1$ resonances, for example, $\Lambda(1405)$, $\Lambda(1670)$, etc. The motivation of the present work is to study the effect of coupling the closed vector meson-baryon (VB) channels to these resonances. To do this, we obtain the PB $\rightarrow$ PB and VB $\rightarrow$ VB amplitudes from the $t$-channel diagrams and the PB $\leftrightarrow$ VB amplitudes are calculated using the Kroll-Ruddermann term where, considering the vector meson dominance phenomena, the photon is replaced by a vector meson. The calculations done within this formalism reveal a very strong coupling of the VB channels to the $\Lambda(1405)$ and $\Lambda(1670)$. In the isospin 1 case, we find evidence for a double pole structure of the $\Sigma(1480)$ which, like the isospin 0 resonances, is also found to couple strongly to the VB channels. The strong coupling of these low-lying resonances to the VB channels can have important implications on certain reactions producing them.

DOI: 10.1103/PhysRevD.84.094018 PACS numbers: 14.20.Gk, 11.10.St, 12.40.Vv

## I. INTRODUCTION

The dynamical generation of baryon resonances in meson-baryon systems has been studied in detail during the past few decades using effective field theories based on chiral symmetry [1–15]. In the early attempts to understand the low-lying baryon resonances, systems made of an octet pseudoscalar meson and an octet baryon were investigated. The resonance which has received a lot of attention in such studies is the $\Lambda(1405)$ [1,3,9,16,17]. Theoretically, the $\Lambda(1405)$ and some states in the nearby energy region are expected to be well studied with the chiral perturbation theory involving unitarization among the coupled channels. The reason being the proximity of these resonance to the threshold of a relevant meson-baryon channels where the chiral perturbation theory can be used as a good guiding principle to determine the hadron-hadron interactions.

Some experimental investigations have been extended to further higher energy regions where some resonances show a large branching ratio to channels consisting of vector mesons (more precisely two or three pseudoscalar mesons with strong correlations to the vector meson quantum numbers). Such states are naturally considered as candidates of dynamically generated states with a vector meson, and several theoretical studies have been made to verify this with a reasonable success [10,12]. In our previous publication also, the importance of the vector meson-baryon interaction in the generation of resonances was pointed out with a more detailed formalism including $s$-, $t$-, $u$-channel diagrams and a contact term originating from the hidden local symmetry Lagrangian [18]. So far, most of the above studies have been carried out by having the pseudoscalar meson-baryon (PB) and vector meson-baryon (VB) channels independently.

Now in general, in the energy region of 1.3–2 GeV, we naturally expect couplings between the PB and VB channels, in particular, when the masses of the PB and VB channels are similar. It is perhaps an aspect of the strong interaction dynamics that we need to systematically include all possible channels. Recently a one loop correction to the VB amplitudes has been made by including PB channels in the intermediate states [19]. The purpose of the present paper is to carry out a full coupled channel calculation.

Here we study strangeness $-1$ baryon resonances dynamically generated from the PB and VB treated as coupled channels. In the investigation dominated by the $S$-wave interaction, as is the case of the present study, such a coupling appears only for $J^P = 1/2^-$ states, while the VB channels alone (uncoupled to PB systems) generate both $J^P = 1/2^-$ and $3/2^-$ states [10,18]. We will not discuss the resonances with the latter quantum numbers in this work since they remain unaffected by coupling PB and VB channels. Within the framework of the low energy expansion of chiral symmetry, PB-VB coupling is provided by an extension of the Kroll-Ruderman (KR) term [20] for the photoproduction of a pseudoscalar meson, by replacing the photon by a vector meson assuming the vector meson dominance. The dynamics of these mesons is well described by the method of hidden local symmetry [21] consistently with chiral symmetry, which is adopted in

*kanchan@rcnp.osaka-u.ac.jp
†amartine@yukawa.kyoto-u.ac.jp
‡kanekoh@rcnp.osaka-u.ac.jp
§nagahiro@rcnp.osaka-u.ac.jp
‖hosaka@rcnp.osaka-u.ac.jp

 

the recent studies of dynamical generation of VB resonances.

The basic ingredients of the present approach are, therefore, the PB $\rightarrow$ PB amplitudes written in terms of the Weinberg-Tomozawa interaction, the VB $\rightarrow$ VB amplitudes obtained from the $t$-channel vector meson exchange interaction, and the PB $\leftrightarrow$ VB transitions acquired via the Kroll-Ruderman type coupling. We do not include a more realistic interaction of the VB channels, because the present work is done to first inspect the kind of and the order of the effect of the PB-VB coupling on the resonances well understood as dynamically generated ones. Our study shows that considering PB and VB as coupled channels brings out interesting results, can generate new resonances and can be very important in understanding the characteristics of the known resonances. This implies that a more quantitative study including more detailed VB interaction should be carried out and we should indeed study it in the near future.

We organize the paper as follows. In Sec. II, as a new information of the present paper, we show briefly how the Kroll-Ruderman type terms for the PB-VB coupling are introduced in the nonlinear sigma model. The basic interactions in the PB and VB channels are also briefly summarized. In Sec. III, we describe the formalism to solve the Bethe-Salpeter equations for PB-VB coupled systems for which we use a cutoff scheme to regularize the loop integrals together with a form factor. This enables us to treat the PB-VB coupling on a reasonable footing when there is some difference in masses of PB and VB channels. We then discuss the results of our calculations in Sec. IV where we show the effects of the PB-VB coupling on the states with strangeness $S = -1$ and $J^P = 1/2^-$. We also pay attention to the behavior of the poles of the scattering amplitudes in the complex plane. In Sec. V, we summarize the findings of the present work.

## II. INTERACTIONS

The purpose of the present paper is to study the PB-VB coupled channel interaction with the motivation of finding dynamical generation of resonances in such systems. For this purpose, it is reasonable to consider that the relative motion in the meson-baryon system is dominantly in the $s$ wave. The new development of this work is the inclusion of the transition between PB and VB systems in the $s$ wave. This is done by using the KR theorem to write the Lagrangian for the $\gamma N \rightarrow \pi N$ process and by replacing the $\gamma$ by a vector meson via the notion of the vector meson dominance. To show this procedure we start with the $\pi N$ Lagrangian from Gell-Mann-Levi's linear sigma model,

$$\mathcal{L}_{\pi N} = \bar{\psi}[i\gamma^\mu \partial_\mu - g_{\pi NN}(\sigma + i\vec{\tau}.\vec{\pi}\gamma_5)]\psi, \quad (1)$$

and define

$$fU_5 = \sigma + i\vec{\tau}.\vec{\pi}\gamma_5, \quad (2)$$

with

$$U_5 = \xi_5^2 = e^{(i\vec{\tau}\cdot\vec{\pi}/f)\gamma_5}, \quad (3)$$

where $f$ is the field length

$$f = (\sigma^2 + \vec{\pi}^2)^{1/2}. \quad (4)$$

Further, considering the nonlinear constraint

$$f^2 \rightarrow f_\pi^2, \quad (5)$$

where $f_\pi = 93$ MeV is the pion decay constant, we can rewrite the Lagrangian in Eq. (1) as

$$\begin{aligned}\mathcal{L}_{\pi N} &= \bar{\psi}[i\gamma^\mu \partial_\mu - g_{\pi NN} f_\pi \xi_5 \xi_5]\psi. \\ &= \bar{N}\xi_5^\dagger i\not{\partial}\xi_5^\dagger N - g_{\pi NN} f_\pi \bar{N}N, \end{aligned} \quad (6)$$

where to obtain the last expression we have defined $\xi_5\psi \equiv N$, $\bar{\psi}\xi_5 \equiv \bar{N}$ (which implies $\psi = \xi_5^\dagger N$, $\bar{\psi} = \bar{N}\xi_5^\dagger$). Subsequently, expanding $\xi_5$ in Eq. (6) up to one pion field and introducing a vector meson field as a gauge boson of the hidden local symmetry

$$i\not{\partial} \longrightarrow i\not{\partial} - g\not{\rho}, \quad (7)$$

we obtain

$$\begin{aligned}\mathcal{L}_{\pi N\rho N} &= -i\frac{g}{2f_\pi}\bar{N}[\pi, \rho^\mu]\gamma_\mu\gamma_5 N \\ &\rightarrow -i\frac{gg_A}{2f_\pi}\bar{N}[\pi, \rho^\mu]\gamma_\mu\gamma_5 N, \end{aligned} \quad (8)$$

where $\pi = \vec{\tau}\cdot\pi$ and $\rho = \vec{\tau}\cdot\frac{\rho}{2}$. In the last expression above we have introduced an arbitrary value of the nucleon axial coupling constant $g_A$, which was unity ($g_A = 1$) in Gell-Mann-Levi's linear sigma model. Thus, Eq. (8) with $g_A$ is the general Lagrangian for $\pi N \rightarrow \rho N$ to the leading order in the soft meson regime.

Next, generalizing the Lagrangian in Eq. (8) for the SU(3) case, we get

$$\begin{aligned}\mathcal{L}_{\text{PBVB}} = \frac{-ig}{2f_\pi}&(F\langle\bar{B}\gamma_\mu\gamma_5[[P, V_\mu], B]\rangle \\ &+ D\langle\bar{B}\gamma_\mu\gamma_5\{[P, V_\mu], B\}\rangle), \end{aligned} \quad (9)$$

where the trace $\langle\ldots\rangle$ has to be calculated in the flavor space and $F = 0.46$, $D = 0.8$ such that $F + D \simeq g_A = 1.26$. The ratio $D/(F + D) \sim 0.63$ here is close to the quark model value of 0.6, and the empirical values of $F$ and $D$ can be found, for example, in Ref. [22].

In our normalization scheme, the SU(3) matrices for the pseudoscalar ($P$) and vector mesons ($V$) are written as

$$V = \frac{1}{2}\begin{pmatrix} \rho^0+\omega & \sqrt{2}\rho^+ & \sqrt{2}K^{*+} \\ \sqrt{2}\rho^- & -\rho^0+\omega & \sqrt{2}K^{*0} \\ \sqrt{2}K^{*-} & \sqrt{2}\bar{K}^{*0} & \sqrt{2}\phi \end{pmatrix},$$
$$P = \begin{pmatrix} \pi^0+\frac{1}{\sqrt{3}}\eta & \sqrt{2}\pi^+ & \sqrt{2}K^+ \\ \sqrt{2}\pi^- & -\pi^0+\frac{1}{\sqrt{3}}\eta & \sqrt{2}K^0 \\ \sqrt{2}K^- & \sqrt{2}\bar{K}^0 & \frac{-2}{\sqrt{3}}\eta \end{pmatrix} \quad (10)$$

and for the baryon ($B$)

$$B = \begin{pmatrix} \frac{1}{\sqrt{6}}\Lambda+\frac{1}{\sqrt{2}}\Sigma^0 & \Sigma^+ & p \\ \Sigma^- & \frac{1}{\sqrt{6}}\Lambda-\frac{1}{\sqrt{2}}\Sigma^0 & n \\ \Xi^- & \Xi^0 & -\sqrt{\frac{2}{3}}\Lambda \end{pmatrix}. \quad (11)$$

The Lagrangian in Eq. (9) leads to the amplitude

$$V_{ij}^{\mathrm{PBVB}} = i\sqrt{3}\frac{g}{2f_\pi}C_{ij}^{\mathrm{PBVB}}, \quad (12)$$

where, using the Kawarabayashi-Suzuki-Riazuddin-Fayazuddin relation, $g = m_\rho/(\sqrt{2}f_\pi) \sim 6$, which from now on we will denote as $g_{\mathrm{KR}}$ (the KR subscript refers to the Kroll-Ruderman coupling). To obtain this value of the coupling we have used $f_\pi = 93$ MeV and the mass of the rho meson ($m_\rho = 770$ MeV). The coefficients $C_{ij}^{\mathrm{PBVB}}$ in Eq. (12) are given in Tables I and II for isospin 0 and 1, respectively.

We obtain the PB $\rightarrow$ PB amplitudes using the Weinberg-Tomozawa (WT) interaction which is well known to give the dominant contribution to the PB scattering. The pseudoscalar-baryon Lagrangian is written as [3]

$$\mathcal{L}_{\mathrm{PB}} = \left\langle \bar{B} i\gamma^\mu \frac{1}{4f_\pi^2}[(\phi\partial_\mu\phi - \partial_\mu\phi\phi)B - B(\phi\partial_\mu\phi - \partial_\mu\phi\phi)] \right\rangle. \quad (13)$$

which reduces to the amplitude of the form

$$V_{ij}^{\mathrm{PB}} = -C_{ij}^{\mathrm{PB}}\frac{1}{4f_\pi^2}(K_1^0 + K_2^0). \quad (14)$$

In Eqs. (14), and throughout this article, $K_1^0$ and $K_2^0$ refer to the energy of the meson in the initial and final state, respectively. Next, the VB amplitudes are determined using the vector-baryon-baryon Lagrangian

$$\mathcal{L}_{\mathrm{VBB}} = -g\{\langle\bar{B}\gamma_\mu[V^\mu, B]\rangle + \langle\bar{B}\gamma_\mu B\rangle\langle V^\mu\rangle\}, \quad (15)$$

and the three vector-meson Lagrangian which can be obtained from

$$\mathcal{L}_{3V} \in -\tfrac{1}{2}\langle V^{\mu\nu}V_{\mu\nu}\rangle. \quad (16)$$

as discussed in detail in Refs. [10,18]. As was shown in Ref. [10], the Lagrangians given by Eqs. (15) and (16) lead to the general form of the vector meson-baryon amplitude:

$$V_{ij}^{\mathrm{VB}} = -C_{ij}^{\mathrm{VB}}\frac{1}{4f_\pi^2}(K_1^0 + K_2^0), \quad (17)$$

which has the structure similar to the PB $\rightarrow$ PB amplitude of Eq. (14).

The coefficients $C_{ij}^{\mathrm{PB}}$ and $C_{ij}^{\mathrm{VB}}$ for the pseudoscalar-baryon and vector-baryon interactions are given in Refs. [3,10]. However, for the sake of completeness, we also list them in Tables III, IV, V, and VI of the present article for isospins 0 and 1.

TABLE I. $C_{ij}^{\mathrm{PBVB}}$ coefficients of the PB $\rightarrow$ VB amplitude [Eq. (12)] in the isospin 0 configuration.

| | $\bar{K}^*N$ | $\omega\Lambda$ | $\rho\Sigma$ | $\phi\Lambda$ | $K^*\Xi$ |
|---|---|---|---|---|---|
| $\bar{K}N$ | $-D-3F$ | $-\frac{1}{\sqrt{6}}(D+3F)$ | $-\sqrt{\frac{3}{2}}(D-F)$ | $\frac{1}{\sqrt{3}}(D+3F)$ | 0 |
| $\pi\Sigma$ | $-\sqrt{\frac{3}{2}}(D-F)$ | 0 | $-4F$ | 0 | $-\sqrt{\frac{3}{2}}(D+F)$ |
| $\eta\Lambda$ | $-\frac{1}{\sqrt{2}}(D+3F)$ | 0 | 0 | 0 | $-\frac{1}{\sqrt{2}}(D-3F)$ |
| $K\Xi$ | 0 | $-\frac{1}{\sqrt{6}}(D-3F)$ | $-\sqrt{\frac{3}{2}}(D+F)$ | $\frac{1}{\sqrt{3}}(D-3F)$ | $D-3F$ |

TABLE II. $C_{ij}^{\mathrm{PBVB}}$ coefficients of the PB $\rightarrow$ VB amplitude [Eq. (12)] in the isospin 1 configuration.

| | $\bar{K}^*N$ | $\rho\Lambda$ | $\rho\Sigma$ | $\omega\Sigma$ | $K^*\Xi$ | $\phi\Sigma$ |
|---|---|---|---|---|---|---|
| $\bar{K}N$ | $D-F$ | $\frac{1}{\sqrt{6}}(D+3F)$ | $-(D-F)$ | $-\frac{1}{\sqrt{2}}(D-F)$ | 0 | $D-F$ |
| $\pi\Sigma$ | $-(D-F)$ | $\sqrt{\frac{2}{3}}2D$ | $-2F$ | 0 | $-(D+F)$ | 0 |
| $\pi\Lambda$ | $\frac{1}{\sqrt{6}}(D+3F)$ | 0 | $\sqrt{\frac{2}{3}}2D$ | 0 | $-\frac{1}{\sqrt{6}}(D-3F)$ | 0 |
| $\eta\Sigma$ | $-\sqrt{\frac{3}{2}}(D-F)$ | 0 | 0 | 0 | $\sqrt{\frac{3}{2}}(D+F)$ | 0 |
| $K\Xi$ | 0 | $-\frac{1}{\sqrt{6}}(D-3F)$ | $-(D+F)$ | $\frac{1}{\sqrt{2}}(D+F)$ | $-(D+F)$ | $-(D+F)$ |

TABLE III. $C_{ij}^{\mathrm{PB}}$ coefficients of the PB $\rightarrow$ PB amplitudes [Eq. (14)] in the isospin 0 configuration.

| | $\bar{K}N$ | $\pi\Sigma$ | $\eta\Lambda$ | $K\Xi$ |
|---|---|---|---|---|
| $\bar{K}N$ | 3 | $-\sqrt{\frac{3}{2}}$ | $\frac{3}{\sqrt{2}}$ | 0 |
| $\pi\Sigma$ | | 4 | 0 | $\sqrt{\frac{3}{2}}$ |
| $\eta\Lambda$ | | | 0 | $-\frac{3}{\sqrt{2}}$ |
| $K\Xi$ | | | | 3 |

TABLE IV. $C_{ij}^{\mathrm{PB}}$ coefficients of the PB $\rightarrow$ PB amplitudes [Eq. (14)] in the isospin 1 configuration.

| | $\bar{K}N$ | $\pi\Sigma$ | $\pi\Lambda$ | $\eta\Sigma$ | $K\Xi$ |
|---|---|---|---|---|---|
| $\bar{K}N$ | 1 | $-1$ | $-\sqrt{\frac{3}{2}}$ | $-\sqrt{\frac{3}{2}}$ | 0 |
| $\pi\Sigma$ | | 2 | 0 | 0 | 1 |
| $\pi\Lambda$ | | | 0 | 0 | $-\sqrt{\frac{3}{2}}$ |
| $\eta\Sigma$ | | | | 0 | $-\sqrt{\frac{3}{2}}$ |
| $K\Xi$ | | | | | 1 |

TABLE V. $C_{ij}^{\mathrm{VB}}$ coefficients of the VB $\rightarrow$ VB amplitudes [Eq. (17)] in the isospin 0 configuration.

| | $\bar{K}^*N$ | $\omega\Lambda$ | $\rho\Sigma$ | $\phi\Lambda$ | $K^*\Xi$ |
|---|---|---|---|---|---|
| $\bar{K}^*N$ | 3 | $\sqrt{\frac{3}{2}}$ | $-\sqrt{\frac{3}{2}}$ | $-\sqrt{3}$ | 0 |
| $\omega\Lambda$ | | 0 | 0 | 0 | $-\sqrt{\frac{3}{2}}$ |
| $\rho\Sigma$ | | | 4 | 0 | $\sqrt{\frac{3}{2}}$ |
| $\phi\Lambda$ | | | | 0 | $\sqrt{3}$ |
| $K^*\Xi$ | | | | | 3 |

TABLE VI. $C_{ij}^{\mathrm{VB}}$ coefficients of the VB $\rightarrow$ VB amplitudes [Eq. (17)] in the isospin 1 configuration.

| | $\bar{K}^*N$ | $\rho\Lambda$ | $\rho\Sigma$ | $\omega\Sigma$ | $K^*\Xi$ | $\phi\Sigma$ |
|---|---|---|---|---|---|---|
| $\bar{K}^*N$ | 1 | $-\sqrt{\frac{3}{2}}$ | $-1$ | $-\frac{1}{\sqrt{2}}$ | 0 | 1 |
| $\rho\Lambda$ | | 0 | 0 | 0 | $-\sqrt{\frac{3}{2}}$ | 0 |
| $\rho\Sigma$ | | | 2 | 0 | 1 | 0 |
| $\omega\Sigma$ | | | | 0 | $-\frac{1}{\sqrt{2}}$ | 0 |
| $K^*\Xi$ | | | | | 1 | 1 |
| $\phi\Sigma$ | | | | | | 0 |

It should be mentioned at this point that it has been shown in Ref. [18] that the contributions obtained from the $u$ channel and a contact interaction coming from the hidden gauge Lagrangian together with the $t$-channel interactions are important in the study of VB systems. In view of the findings of Ref. [18], in principle, considering the $t$-channel exchange alone would lead to incomplete information. However, first, the purpose of the present work is to study the properties of strangeness $-1$ low energy resonances, like $\Lambda(1405)$, when the heavier VB channels are coupled to the PB systems. And second, we cannot *a priori* know if the PB-VB coupling would offer important new information. We, thus, start with a simplified model where the VB $\rightarrow$ VB amplitudes are obtained from the $t$ channel, while neglecting other contributions as done in a previous study of the VB systems [10].

In principle, there is also some room for improvement in the case of the PB interaction, for example, a baryon exchange in the $s$ and $u$ channel has been considered in Ref. [9] or the next-to-leading-order amplitudes in the chiral perturbation theory ($\chi$PT) have been considered in Ref. [23]. In the former study the contribution from the $s$- and $u$-channel diagrams was found to be of the order of 20% of the WT interaction, a result consistent with the chiral counting in the nonrelativistic limit, which is the case, in particular, near the threshold region. However, that correction is much smaller than the one that arises in the VB systems by including the diagrams other than the $t$ channel. In Ref. [23], in addition to the $\Lambda(1405)$ and $\Lambda(1670)$, which are found in studies involving leading-order $\chi$PT, several other resonances were found as dynamically generated ones: $\Lambda$ (1800), $\Sigma$ (1480), $\Sigma$ (1620) and $\Sigma$ (1750). Some of these resonances, like, the $\Lambda$ (1800) and $\Sigma$ (1750) have been also found in VB systems studied using the $t$-channel interactions [10,18]. Also, the spin parity of the $\Sigma$ (1620) is controversial in nature as stated in Ref. [24]. It has been found to be a $1/2^+$ resonance in some of the recent works [25,26]. These findings indicate that more than one interpretation should be included to better clarify the nature of the strangeness $-1$ resonances in the energy region: 1700–2000 MeV, which we believe is an important direction to be considered in future works. Besides we would like to keep the minimum number of parameters in the present study and focus our attention to the low-lying resonances in this work. We thus rely on the WT interaction only to obtain the PB $\rightarrow$ PB amplitudes.

We would like to point out that the VB interaction [Eq. (17)] determined from the $t$-channel exchange gives rise to spin independent amplitudes. Thus, the amplitudes obtained and the poles found in the VB system possess spin $1/2$ and $3/2$. However, the coupling of the PB to VB channels in $s$ wave, as is the case of the present study, would affect only the spin $1/2$ amplitudes. Consequently, only the results obtained for spin $1/2$ meson-baryon systems will be discussed in the present work.

Finally, the entire set of interactions can be summarized as shown in Table VII.

TABLE VII. A summary of all the interactions.

| $V_{ij}$ | VB | PB |
|---|---|---|
| VB | $-C_{ij}^{\mathrm{VB}}\frac{1}{4f_\pi^2}(K_1^0+K_2^0)$ | $-i\sqrt{3}\frac{g_{\mathrm{KR}}}{2f_\pi}C_{ij}^{\mathrm{PBVB}}$ |
| PB | $i\sqrt{3}\frac{g_{\mathrm{KR}}}{2f_\pi}C_{ij}^{\mathrm{PBVB}}$ | $-C_{ij}^{\mathrm{PB}}\frac{1}{4f_\pi^2}(K_1^0+K_2^0)$ |

## III. FORMALISM

### A. Solving coupled channel equations

In the previous section we have discussed the basic interactions for PB-VB coupled systems. Using the tree level amplitudes, summarized in Table VII, as the kernels $V$, we solve the Bethe-Salpeter equation

$$T = V + VGT, \tag{18}$$

which, for a single meson-baryon channel case, can be explicitly written as

$$T(k_1,k_2) = V(k_1,k_2) + 2Mi\int \frac{d^4q}{(2\pi)^4} \times \frac{V(k_1,q)T(q,k_2)}{(q^2-m^2+i\epsilon)((P-q)^2-M^2+i\epsilon)}, \tag{19}$$

where $k_1(k_2)$ is the four momentum of the meson in the initial (final) state, $m$, $M$ (here and throughout this article) are the meson and baryon masses, respectively, and $P$ is the total four momentum of the system. It has been shown in earlier works (for example, in Refs. [3,27]) that in the low energy studies of two hadron systems based on chiral unitary dynamics, $V$ and $T$ can be factorized out of the loop integral in Eq. (19). This simplifies the integral Bethe-Salpeter equation to an algebraic one since the calculation of the loop integral involves only the $G$ function

$$G = 2Mi\int \frac{d^4q}{(2\pi)^4} \frac{1}{(q^2-m^2+i\epsilon)((P-q)^2-M^2+i\epsilon)}. \tag{20}$$

These loop functions are divergent in nature and one either calculates them by using the dimensional regularization method or the cutoff method. The former scheme involves subtraction constants as the parameters, while in the latter case a cutoff is used. One could use any of the two methods although sometimes one of them can be more suitable to a particular case. For example, based on the behavior of the loop calculated with a cutoff, in Ref. [28] it has been discussed how dynamically generated states can be studied while excluding the contribution from other possible states to the amplitudes. It is worth discussing this issue in some detail before going ahead.

### B. Calculation of the loops

The aim of the present work is to study the effect of the VB channels on the poles corresponding to the dynamically generated states found in the PB systems. Following the discussions made in Ref. [28], from the time independent perturbation theory, one would expect, up to the second order, a correction to the mass of a resonance to be proportional to

$$\Delta E \propto \sum_q \frac{|\langle \mathrm{VB}|V|\mathrm{PB}\rangle|^2}{E-E(q)}, \tag{21}$$

where $E$ is the total energy of the unperturbed system, and $E(q)$ is the energy of an intermediate state labeled by $q$. The contribution of the above equation should be negative for the closed channels, for which $E(q) > E$, and one would näively expect a pole to shift to lower energies if a coupling to a closed channel is introduced. From these basics one can discuss the behavior of the $G$ function [Eq. (20)], though it is mathematically divergent [28]. It should be recalled that the divergent nature of this function arises if one assumes the hadrons to be point particles. It would be convergent if the extended spatial structure of the hadrons were taken into account. Thus, keeping in mind that the regularization methods effectively correspond to considering the finite structure of the hadrons, it is possible to discuss the features of the $G$ function, intuitively, from the physics point of view.

Let us now look at the loop function calculated with different regularizing schemes: the cutoff and the dimensional regularization. As an example, we show the real part of the loop for the $\bar{K}^*N$ channel in the left panel of Fig. 1.

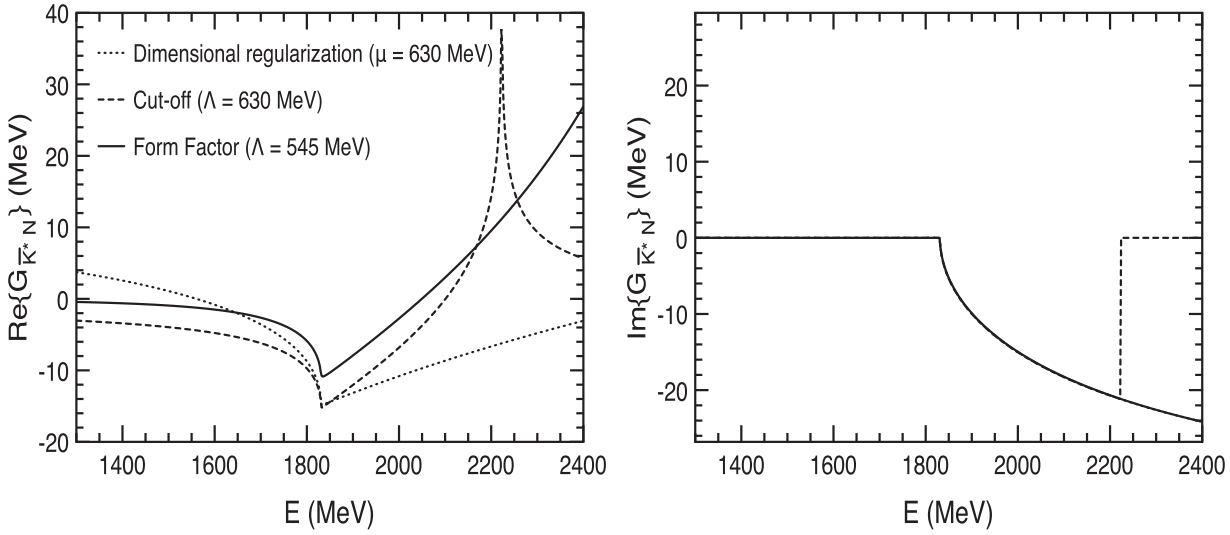


FIG. 1. Real (left panel) and imaginary (right panel) parts of the loop calculated for the $\bar{K}^*N$ channel on the real energy axis.

The dotted line shows the result of the calculation done by using the dimensional regularization method with a subtraction constant $a_{\bar{K}^*N} = -2$ and the dashed curve shows the loop calculated by using a cutoff of 630 MeV. This value of the cutoff is chosen such that the two schemes give the same result at the threshold. It is interesting to see that real part of the loop obtained within the dimensional regularization scheme changes the sign and becomes large and positive far below the threshold unlike the one obtained by the cutoff method. Proceeding further with our study of the PB-VB coupled systems by calculating the loops with the dimensional regularization scheme, we obtained some inconsistent results, for example, we found that the $\Lambda(1405)$ poles moved to higher energies due to the coupling to the VB channels. This is contrary to what we would expect from the standard quantum mechanical two level problem where the lower energy state is pushed further down in energy by the coupling to the higher energy state (which would correspond to the VB states in the present case). A discussion on some problems related to the loop calculated in the dimensional regularization scheme has also been made in Ref. [29], where the authors find that unphysical poles get developed with a repulsive potential in their study due to the positive real part of the loop far below the threshold. Thus for the purpose of studying dynamically generated or molecularlike states in the PB-VB coupled systems, we find that the loop calculated with the cutoff method is more suitable. Hence, we proceed by using a cutoff to obtain the loops. However, the loops calculated in this way possess sharp structures (see the dashed lines in Fig. 1 near 2.2 GeV) precisely due to the use of a sharp cutoff and additionally suffer other limitations like violating the unitarity conditions. This would limit our calculations to the energies below the one corresponding to the cutoff momentum. In order to solve this problem, we multiply the loops by a form factor

$$\mathcal{F} = e^{-((q^2-q_{on}^2)/\Lambda^2)}, \tag{22}$$

and extend the upper limit of the loop integral to infinity, which would correspond to taking the fact into account that the hadrons possess an extended spatial structure. In Eq. (22), $q_{on}$ is the on-shell momentum in the center of mass system of the propagating meson-baryon pair and $\Lambda$ is the cutoff momentum. The loop

$$G = \int_0^\infty \frac{d^3q}{(2\pi)^3} \frac{1}{2E_1(\vec{q}, m)} \frac{2M}{2E_2(\vec{q}, M)} \times \frac{\mathcal{F}}{E - E_1(\vec{q}, m) - E_2(\vec{q}, M)}, \tag{23}$$

calculated in the nonrelativistic approximation, and using a cutoff of 545 MeV and the form factor of Eq. (22), is shown as the solid curve in Fig. 1. We would like to emphasize that the loop calculated in this way satisfies the unitarity conditions. In Eq. (23), $E$ refers to the total energy of the meson-baryon system, which corresponds to the $E$ in Eq. (21). The loop shown in Fig. 1 has been calculated using a cutoff 545 MeV because, as we shall show later, this value gives very similar amplitudes as those obtained by the dimensional regularization method. We further show that the behavior of the loops, calculated using Eq. (23), in the complex plane is as expected. For this we depict the loop function on the Riemann sheets connected to the physical scattering line, for the $\bar{K}^*N$ channel, in Fig. 2.

In concluding the discussion of the loops, we would like to mention that in the case of systems involving vector mesons, which can possess large widths sometimes, like the $\rho$ and the $K^*$ mesons, we calculate the loop given by Eq. (23), by convoluting them over the mass range of these mesons as discussed in Ref. [10].

Further, to test the reliability of our method to calculate the loop, we obtain the amplitudes for the uncoupled PB and VB systems with the loop given by Eq. (23). We found that in order to reproduce the results of previous uncoupled studies of PB and VB systems, which agree with the available experimental data, we need to use a cutoff

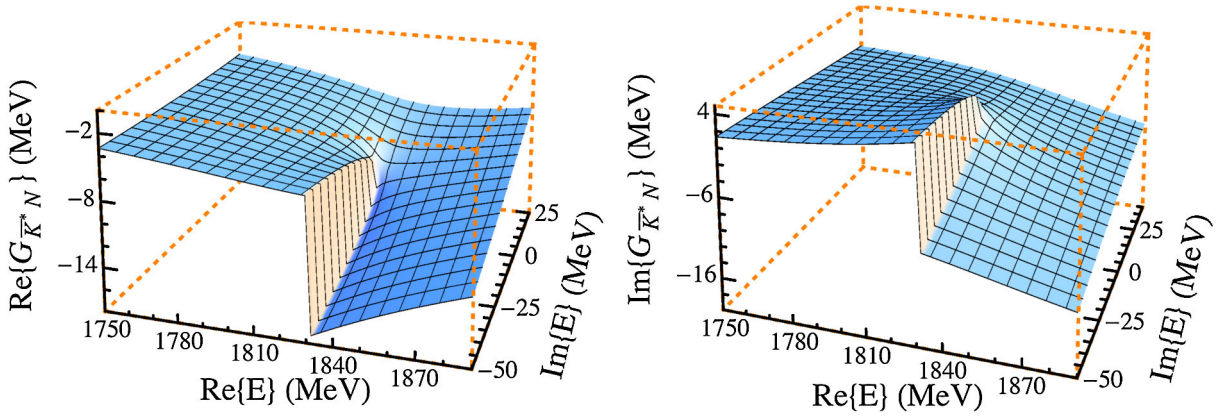


FIG. 2 (color online). Real (left panel) and imaginary (right panel) parts of the loop [Eq. (23)] calculated for the $\bar{K}^*N$ channel on the Riemann sheets connected to the physical scattering line.

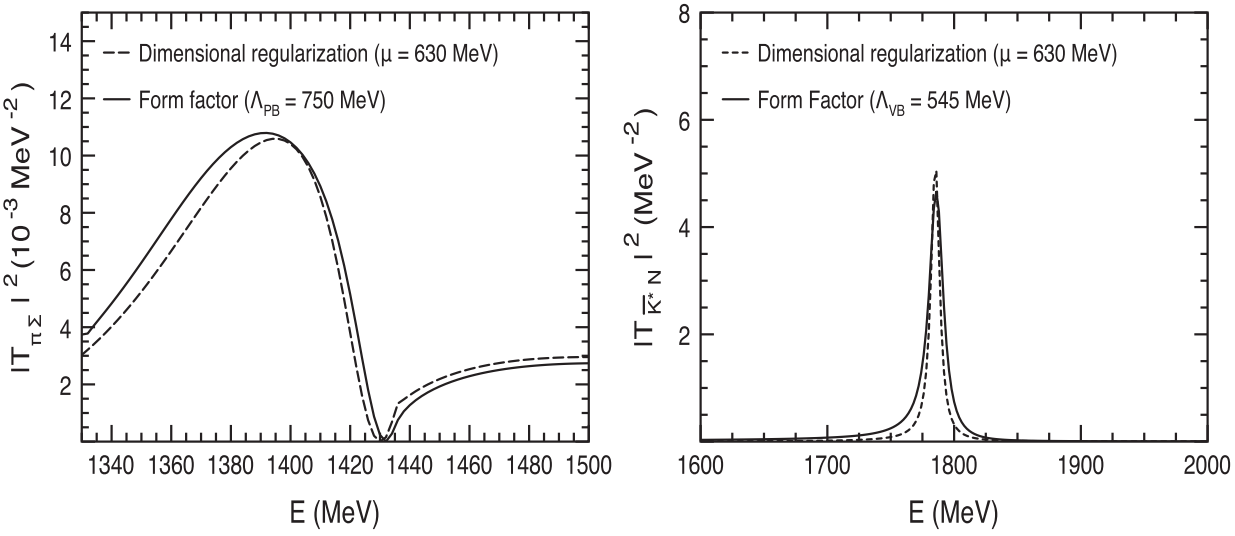


FIG. 3. Squared amplitude of the $\pi\Sigma$ (left panel) and $\bar{K}^*N$ (right panel) channels obtained by considering uncoupled PB-VB systems. The dashed and solid lines are the results of the calculation done with the loops obtained with the dimensional regularization and cutoff method [Eq. (23)], respectively.

$\Lambda_{VB} = 545$ MeV for the VB and $\Lambda_{PB} = 750$ MeV for PB systems. Using these two parameters, we have found that we can reproduce all of the previous results of Refs. [3,10] reasonably well. As an example, in Fig. 3, we show a comparison of the $\pi\Sigma$ and $\bar{K}^*N$ amplitudes obtained by solving the coupled channel Bethe-Salpeter equation with the loops calculated by using the dimensional regularization method with the subtraction constants taken from Refs. [10,30] and by using the cutoff method involving a form factor [Eq. (23)]. As can be seen in Fig. 3, the two results are satisfactorily similar. In the following, we will also discuss the poles obtained in the uncoupled PB-VB systems, along with their coupling to the related channels, in the calculations done with the loops obtained by using Eq. (23).

## IV. RESULTS AND DISCUSSIONS

### A. Coupled PB-VB systems in isospin 0

Let us first study the total isospin zero systems, in which case we have nine (four PB and five VB) coupled channels: $\bar{K}N$, $\pi\Sigma$, $\eta\Lambda$, $K\Xi$, $\bar{K}^*N$, $\omega\Lambda$, $\rho\Sigma$, $\phi\Lambda$, and $K^*\Xi$. We first obtain the amplitudes keeping the coupling between the PB and VB channels, $g_{KR}$, as zero, i.e., treating them as uncoupled systems, and by calculating the loops [Eq. (23)] using the cutoffs $\Lambda_{VB} = 545$ MeV for the VB loops and $\Lambda_{PB} = 750$ MeV for the PB case. The amplitudes obtained on the real axis in this case are shown as the dotted curves in Figs. 4 and 5. The corresponding poles are listed in the second column of Tables VIII, IX, X, XI, XII, and XIII. There are six poles found in this case: two related to the $\Lambda(1405)$, one to the $\Lambda(1670)$ and the rest three are spin degenerate in nature due to the spin-independent form of the vector-baryon interaction. Together, Figs. 4 and 5 and Tables VIII, IX, X, XI, XII, and XIII show that the results obtained with $g_{KR} = 0$ are in good agreement with the ones reported in Refs. [3,10].

Next, we change the coupling between the PB and VB channels, $g_{KR}$, from zero to its maximum value which is 6 and show how the amplitudes and poles found in the uncoupled PB-VB systems ($g_{KR} = 0$) change their behavior due to the coupling between these channels. Figs. 4 and 5 show the isospin 0 PB, VB amplitudes for $g_{KR} = 0$, 1.5, 3, and 6 and Tables VIII, IX, X, XI, XII, and XIII show the poles found by changing $g_{KR}$ gradually from 0 to 6 in steps of 1. In the following subsections, we discuss each of these poles separately.

#### *1. Two poles of the* $\Lambda(1405)$ *resonance:*

As shown in Tables VIII and IX, we find two poles for the $\Lambda(1405)$ resonance when $g_{KR} = 0$ at: $1377 - i63$ MeV and $1430 - i15$ MeV. The former one couples strongly to $\pi\Sigma$ and the latter one to $\bar{K}N$ in agreement with the findings of Refs. [16,17].

By switching on the coupling between PB-VB channels, but keeping it small, i.e., $g_{KR} = 1$, we see that the couplings remains very similar for the PB channels while a small coupling for the VB channels develops. On increasing $g_{KR}$ merely to 2, we find that the coupling of the lower pole to the closed VB channels $\rho\Sigma$ and $K^*\Xi$ becomes similar to those of the $\bar{K}N$ and $\pi\Sigma$ channels and the coupling of the higher pole ($1430 - i15$ MeV) to $\bar{K}^*N$ becomes comparable to that of $\bar{K}N$. If $g_{KR}$ is fixed to half of its strength (which is 3), the couplings of the two $\Lambda(1405)$ poles to the PB channels remain almost unchanged but increase for the VB channels.

The full strength of $g_{KR}$ leads to a slight shift in the masses and widths of the two poles, we find them at

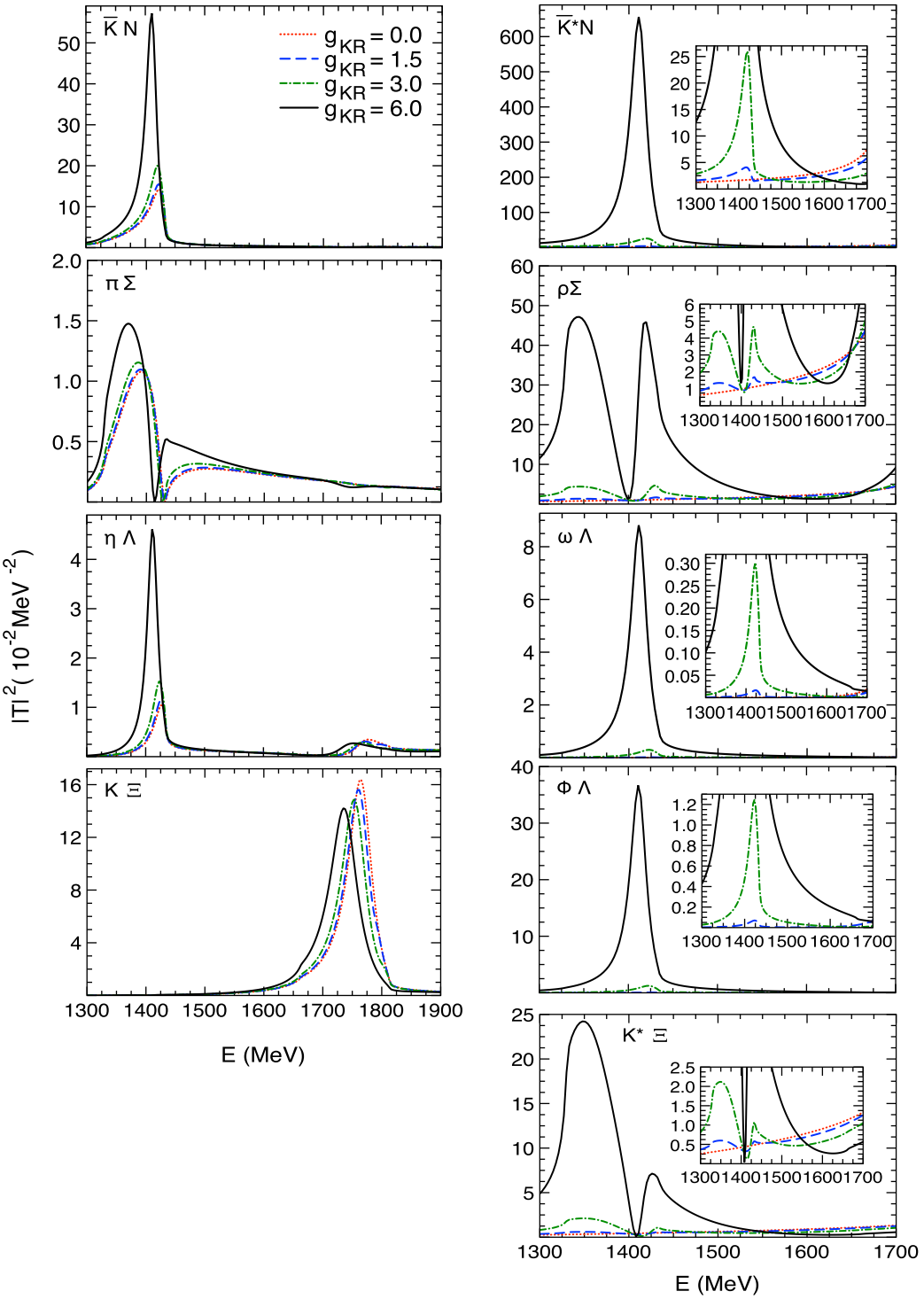


FIG. 4 (color online). Isospin 0 amplitudes of the PB and VB systems for the energy $\leq 1900$ MeV. The purpose of the inset figures is to show the structure of the amplitudes hidden in the corresponding large figures due to their smaller magnitudes.

$1363 - i56$ MeV and $1412 - i11$ MeV which couple much stronger to some VB channels than to PB. The coupling of the pole at $1363 - i56$ MeV to $\rho\Sigma$ and $K^*\Xi$ is twice the one to $\pi\Sigma$ while the latter coupling is very similar to the one obtained for $g_{\rm KR} = 0$. The pole at $1412 - i11$ MeV turns out to couple strongly to the $\bar{K}^*N$ channel, almost 2 times more than to the $\bar{K}N$ channel. Interestingly, since neither the pole positions nor the coupling of the $\Lambda(1405)$ poles to PB are altered much by the inclusion of VB as coupled channels, the amplitudes for the PB channels on the real energy axis continue looking very similar, except for a change in the strength, as shown

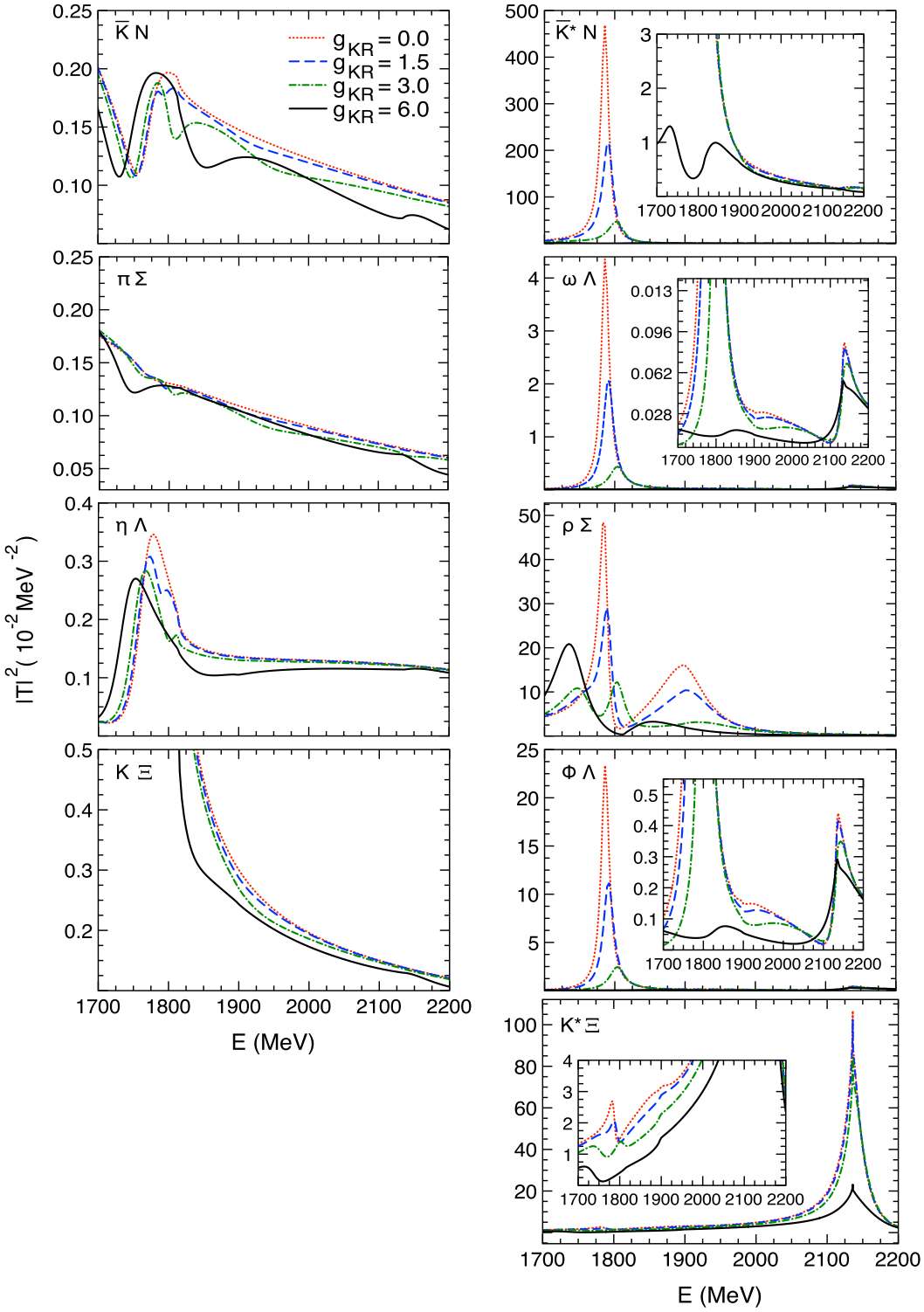


FIG. 5 (color online). Isospin 0 amplitudes of the PB and VB systems for the energy region 1700–2200 MeV. The inset figures here have the same objective as those in Fig. 4.

in Fig. 4 (left column). The amplitude for the $\pi\Sigma$ channel, for which data is available, changes only slightly. Though it depicts one curious feature, that is, a zero at the mass of the higher pole at $g_{\mathrm{KR}} = 6$, unlike the amplitude calculated with $g_{\mathrm{KR}} = 0$. Our results show that although the PB channels can generate the $\Lambda(1405)$ and the available data can be explained with this information, a better understanding of the structure of the $\Lambda(1405)$ requires the consideration of the VB channels. The (diagonal) amplitudes for the VB channels are also shown in Fig. 4 (right

TABLE VIII. $g^i$ couplings for the lower mass pole of the $\Lambda(1405)$ to PB and VB channels for different strengths of the coupling between PB-VB systems. Note that the couplings have been listed with a precision to the first decimal place in this (and subsequent) table(s), which leads to rounding off of a number smaller than 0.05 to 0.0 for $g_{\rm KR} > 0$.

| PB-VB coupling: $g_{\rm KR}$ | 0 | 1 | 2 | 3 | 4 | 5 | 6 |
|---|---|---|---|---|---|---|---|
| $M_R - i\Gamma/2$ (MeV) $\rightarrow$ | $1377 - i63$ | $1376 - i63$ | $1374 - i62$ | $1372 - i61$ | $1368 - i59$ | $1363 - i56$ | $1357 - i53$ |
| Channels $\downarrow$ | Couplings ($g^i$) of the poles to the different channels | | | | | | |
| $\bar{K}N$ | $1.4 - i1.6$ | $1.4 - i1.6$ | $1.4 - i1.6$ | $1.3 - i1.6$ | $1.3 - i1.5$ | $1.2 - i1.5$ | $1.1 - i1.4$ |
| $\pi\Sigma$ | $-2.3 + i1.4$ | $-2.3 + i1.5$ | $-2.2 + i1.5$ | $-2.3 + i1.4$ | $-2.3 + i1.4$ | $-2.2 + i1.4$ | $-2.2 + i1.4$ |
| $\eta\Lambda$ | $0.2 - i0.7$ | $0.2 - i0.6$ | $0.2 - i0.6$ | $0.1 - i0.6$ | $0.1 - i0.6$ | $0.1 - i0.6$ | $0.1 - i0.6$ |
| $K\Xi$ | $-0.4 + i0.4$ | $-0.4 + i0.4$ | $-0.4 + i0.4$ | $-0.5 + i0.4$ | $-0.5 + i0.4$ | $-0.5 + i0.4$ | $-0.6 + i0.4$ |
| $\bar{K}^*N$ | $0.0 + i0.0$ | $-0.4 + i0.1$ | $-0.7 + i0.2$ | $-1.1 + i0.3$ | $-1.4 + i0.5$ | $-1.6 + i0.5$ | $-1.7 + i0.7$ |
| $\omega\Lambda$ | $0.0 + i0.0$ | $-0.2 - i0.1$ | $-0.3 - i0.1$ | $-0.4 - i0.2$ | $-0.6 - i0.2$ | $-0.7 - i0.3$ | $-0.7 - i0.3$ |
| $\rho\Sigma$ | $0.0 + i0.0$ | $0.1 + i1.2$ | $0.3 + i2.3$ | $0.4 + i3.6$ | $0.7 + i4.7$ | $0.9 + i5.7$ | $1.3 + i6.8$ |
| $\phi\Lambda$ | $0.0 + i0.0$ | $0.2 + i0.1$ | $0.4 + i0.2$ | $0.6 + i0.3$ | $0.8 + i0.3$ | $0.9 + i0.4$ | $1.0 + i0.5$ |
| $K^*\Xi$ | $0.0 + i0.0$ | $0.2 + i1.0$ | $0.4 + i2.0$ | $0.5 + i3.0$ | $0.7 + i3.9$ | $0.9 + i4.8$ | $1.3 + i5.7$ |

TABLE IX. $g^i$ couplings for the higher mass pole of the $\Lambda(1405)$.

| PB-VB coupling: $g_{\rm KR}$ | 0 | 1 | 2 | 3 | 4 | 5 | 6 |
|---|---|---|---|---|---|---|---|
| $M_R - i\Gamma/2$ (MeV) $\rightarrow$ | $1430 - i15$ | $1430 - i15$ | $1428 - i15$ | $1426 - i14$ | $1422 - i14$ | $1418 - i12$ | $1412 - i11$ |
| Channels $\downarrow$ | Couplings ($g^i$) of the poles to the different channels | | | | | | |
| $\bar{K}N$ | $2.4 + i1.1$ | $2.4 + i1.1$ | $2.4 + i1.0$ | $2.5 + i0.9$ | $2.6 + i0.8$ | $2.7 + i0.7$ | $2.8 + i0.5$ |
| $\pi\Sigma$ | $-0.2 - i1.4$ | $-0.2 - i1.3$ | $-0.2 - i1.3$ | $-0.2 - i1.3$ | $-0.2 - i1.2$ | $-0.2 - i1.2$ | $-0.2 - i1.1$ |
| $\eta\Lambda$ | $1.3 + i0.3$ | $1.4 + i0.3$ | $1.4 + i0.3$ | $1.4 + i0.2$ | $1.4 + i0.2$ | $1.5 + i0.1$ | $1.5 + i0.1$ |
| $K\Xi$ | $0.0 - i0.3$ | $0.0 - i0.3$ | $0.0 - i0.3$ | $0.0 - i0.3$ | $0.0 - i0.3$ | $0.0 - i0.3$ | $0.0 - i0.3$ |
| $\bar{K}^*N$ | $0.0 + i0.0$ | $0.1 - i0.9$ | $0.1 - i1.8$ | $0.2 - i2.7$ | $0.1 - i3.6$ | $0.0 - i4.5$ | $-0.1 - i5.3$ |
| $\omega\Lambda$ | $0.0 + i0.0$ | $0.1 - i0.3$ | $0.1 - i0.6$ | $0.2 - i0.9$ | $0.2 - i1.2$ | $0.2 - i1.5$ | $0.2 - i1.8$ |
| $\rho\Sigma$ | $0.0 + i0.0$ | $-0.5 - i0.3$ | $-0.9 - i0.6$ | $-1.3 - i0.9$ | $-1.7 - i1.2$ | $-2.1 - i1.4$ | $-2.4 - i1.6$ |
| $\phi\Lambda$ | $0.0 + i0.0$ | $-0.1 + i0.4$ | $-0.2 + i0.9$ | $-0.2 + i1.3$ | $-0.3 + i1.7$ | $-0.3 + i2.2$ | $-0.3 + i2.6$ |
| $K^*\Xi$ | $0.0 + i0.0$ | $-0.4 - i0.1$ | $-0.8 - i0.3$ | $-1.1 - i0.4$ | $-1.5 - i0.5$ | $-1.7 - i0.5$ | $-2.0 - i0.5$ |

TABLE X. $g^i$ couplings for the pole related to $\Lambda(1670)$.

| PB-VB coupling: $g_{\rm KR}$ | 0 | 1 | 2 | 3 | 4 | 5 | 6 |
|---|---|---|---|---|---|---|---|
| $M_R - i\Gamma/2$ (MeV) $\rightarrow$ | $1767 - i25$ | $1766 - i25$ | $1763 - i25$ | $1759 - i25$ | $1754 - i26$ | $1749 - i27$ | $1744 - i28$ |
| Channels $\downarrow$ | Couplings ($g^i$) of the poles to the different channels | | | | | | |
| $\bar{K}N$ | $0.2 - i0.5$ | $0.2 - i0.5$ | $0.2 - i0.6$ | $0.2 - i0.6$ | $0.2 - i0.6$ | $0.2 - i0.6$ | $0.3 - i0.6$ |
| $\pi\Sigma$ | $0.1 + i0.2$ | $0.1 + i0.2$ | $0.1 + i0.2$ | $0.1 + i0.2$ | $0.1 + i0.3$ | $0.1 + i0.3$ | $0.1 + i0.3$ |
| $\eta\Lambda$ | $-1.0 + i0.3$ | $-1.0 + i0.3$ | $-1.0 + i0.3$ | $-1.0 + i0.3$ | $-1.0 + i0.3$ | $-1.0 + i0.3$ | $-1.0 + i0.3$ |
| $K\Xi$ | $3.2 + i0.3$ | $3.2 + i0.3$ | $3.2 + i0.3$ | $3.2 + i0.3$ | $3.3 + i0.3$ | $3.3 + i0.3$ | $3.4 + i0.2$ |
| $\bar{K}^*N$ | $0.0 + i0.0$ | $0.0 + i0.4$ | $-0.1 + i0.6$ | $-0.2 + i0.8$ | $-0.2 + i0.9$ | $-0.3 + i1.0$ | $-0.3 + i1.1$ |
| $\omega\Lambda$ | $0.0 + i0.0$ | $0.0 + i0.1$ | $0.1 + i0.1$ | $0.1 + i0.1$ | $0.1 + i0.1$ | $0.1 + i0.0$ | $0.1 - i0.1$ |
| $\rho\Sigma$ | $0.0 + i0.0$ | $0.0 - i0.8$ | $0.0 - i1.6$ | $0.0 - i2.2$ | $0.1 - i2.8$ | $0.2 - i3.2$ | $0.3 - i3.5$ |
| $\phi\Lambda$ | $0.0 + i0.0$ | $-0.1 - i0.1$ | $-0.1 - i0.1$ | $-0.1 - i0.1$ | $-0.1 - i0.1$ | $-0.1 - i0.0$ | $-0.2 + i0.1$ |
| $K^*\Xi$ | $0.0 + i0.0$ | $0.0 - i0.3$ | $0.1 - i0.6$ | $0.2 - i0.8$ | $0.3 - i1.0$ | $0.4 - i1.1$ | $0.5 - i1.2$ |

column), where the presence of the two poles of the $\Lambda(1405)$ can be seen.

### *2.* $\Lambda(1670)$*:*

A resonance around 1700 MeV, which was interpreted as a $K\Xi$ bound state, was found in a study of PB systems [30]. The pole associated to this resonance was found to be very sensitive to the subtraction constant for the $K\Xi$ channel ($a_{K\Xi}$), it appeared at $1680 - i20$ MeV with $a_{K\Xi} = -2.67$ and at $1708 - i21$ MeV with $a_{K\Xi} = -2.52$. In our case, using the same cutoffs throughout our study ($\Lambda_{\rm VB} = 545$ MeV for the VB systems and $\Lambda_{\rm PB} = 750$ MeV for

TABLE XI. $g^i$ couplings of the $P_i$ pole as a function of $g_{\rm KR}$.

| PB-VB coupling: $g_{\rm KR}$ | 0 | 1 | 2 | 3 | 4 | 5 | 6 |
|---|---|---|---|---|---|---|---|
| $M_R - i\Gamma/2$ (MeV) $\rightarrow$ | $1795 - i0$ | $1797 - i0.5$ | $1802 - i2$ | $1812 - i4$ | $1822 - i6.5$ | $\cdots$ | $1844 - i94$ |
| Channels $\downarrow$ | Couplings ($g^i$) of the poles to the different channels | | | | | | |
| $\bar{K}N$ | $0.0 + i0.0$ | $-0.1 + i0.0$ | $-0.2 + i0.1$ | $-0.3 + i0.1$ | $-0.4 + i0.0$ | $\cdots$ | $-1.2 - i0.5$ |
| $\pi\Sigma$ | $0.0 + i0.0$ | $-0.1 + i0.0$ | $-0.1 + i0.1$ | $-0.1 + i0.1$ | $-0.1 + i0.0$ | $\cdots$ | $-0.4 - i0.3$ |
| $\eta\Lambda$ | $0.0 + i0.0$ | $-0.1 - i0.0$ | $-0.2 - i0.1$ | $-0.2 - i0.1$ | $-0.3 - i0.1$ | $\cdots$ | $-0.6 - i0.2$ |
| $K\Xi$ | $0.0 + i0.0$ | $0.1 + i0.2$ | $0.0 + i0.3$ | $0.0 + i0.4$ | $0.1 + i0.3$ | $\cdots$ | $0.4 + i0.3$ |
| $\bar{K}^*N$ | $3.8 - i0.0$ | $3.7 + i0.0$ | $3.4 + i0.1$ | $2.9 + i0.3$ | $2.3 + i0.5$ | $\cdots$ | $1.6 - i0.8$ |
| $\omega\Lambda$ | $1.2 - i0.0$ | $1.2 + i0.0$ | $1.1 + i0.0$ | $0.9 + i0.1$ | $0.7 + i0.1$ | $\cdots$ | $0.7 - i0.1$ |
| $\rho\Sigma$ | $-1.9 - i0.0$ | $-1.9 + i0.0$ | $-1.8 + i0.1$ | $-1.9 + i0.2$ | $-2.0 + i0.1$ | $\cdots$ | $-5.4 + i0.0$ |
| $\phi\Lambda$ | $-1.8 - i0.0$ | $-1.8 - i0.0$ | $-1.6 - i0.1$ | $-1.4 - i0.1$ | $-1.1 - i0.2$ | $\cdots$ | $-1.2 + i0.1$ |
| $K^*\Xi$ | $-0.6 - i0.0$ | $-0.5 + i0.0$ | $-0.5 + i0.0$ | $-0.5 + i0.1$ | $-0.5 + i0.0$ | $\cdots$ | $-1.2 - i0.2$ |

TABLE XII. $g^i$ couplings for the $P_{ii}$ pole as a function of $g_{\rm KR}$. The sign ** in this table indicates the unphysical nature of a pole.

| PB-VB coupling: $g_{\rm KR}$ | 0 | 1 | 2 | 3 | 4 | 5 | 6 |
|---|---|---|---|---|---|---|---|
| $M_R - i\Gamma/2$ (MeV) $\rightarrow$ | $1923 - i4$ | $1926 - i6$ | $1934 - i10$ | $1948 - i16$ | $1969 - i11^{**}$ | $2012 - i6^{**}$ | $2090 - i14^{**}$ |
| Channels $\downarrow$ | Couplings ($g^i$) of the poles to the different channels | | | | | | |
| $\bar{K}N$ | $0.0 + i0.0$ | $-0.1 + i0.1$ | $-0.2 + i0.1$ | $-0.3 + i0.2$ | $\cdots$ | $\cdots$ | $\cdots$ |
| $\pi\Sigma$ | $0.0 + i0.0$ | $-0.1 + i0.0$ | $-0.2 + i0.1$ | $-0.3 + i0.1$ | $\cdots$ | $\cdots$ | $\cdots$ |
| $\eta\Lambda$ | $0.0 + i0.0$ | $0.0 + i0.0$ | $0.0 + i0.0$ | $0.0 + i0.1$ | $\cdots$ | $\cdots$ | $\cdots$ |
| $K\Xi$ | $0.0 + i0.0$ | $-0.1 - i0.0$ | $-0.2 - i0.1$ | $-0.3 - i0.3$ | $\cdots$ | $\cdots$ | $\cdots$ |
| $\bar{K}^*N$ | $0.1 - i0.5$ | $0.0 - i0.5$ | $0.0 - i0.6$ | $-0.1 - i0.7$ | $\cdots$ | $\cdots$ | $\cdots$ |
| $\omega\Lambda$ | $0.3 - i0.2$ | $0.3 - i0.2$ | $0.3 - i0.2$ | $0.4 - i0.3$ | $\cdots$ | $\cdots$ | $\cdots$ |
| $\rho\Sigma$ | $3.7 + i0.2$ | $3.6 + i0.2$ | $3.2 + i0.4$ | $2.6 + i0.9$ | $\cdots$ | $\cdots$ | $\cdots$ |
| $\phi\Lambda$ | $-0.5 + i0.3$ | $-0.5 + i0.3$ | $-0.5 + i0.3$ | $-0.5 + i0.4$ | $\cdots$ | $\cdots$ | $\cdots$ |
| $K^*\Xi$ | $1.0 + i0.0$ | $0.9 + i0.0$ | $0.7 + i0.1$ | $0.3 + i0.3$ | $\cdots$ | $\cdots$ | $\cdots$ |

TABLE XIII. $g^i$ couplings for the $P_{iii}$ pole as a function of $g_{\rm KR}$.

| PB-VB coupling: $g_{\rm KR}$ | 0 | 1 | 2 | 3 | 4 | 5 | 6 | |
|---|---|---|---|---|---|---|---|---|
| $M_R - i\Gamma/2$ (MeV) $\rightarrow$ | $2138 - i21$ | $2138 - i21$ | $2140 - i22$ | $2143 - i23$ | $2149 - i25$ | $2159 - i33$ | $2151 - i119$ | $2160 - i73$ |
| Channels $\downarrow$ | Couplings ($g^i$) of the poles to the different channels | | | | | | | |
| $\bar{K}N$ | $0.0 + i0.0$ | $0.0 + i0.0$ | $0.0 + i0.0$ | $-0.1 + i0.0$ | $-0.1 + i0.0$ | $-0.1 + i0.2$ | $1.3 - i0.3$ | $0.2 + i0.9$ |
| $\pi\Sigma$ | $0.0 + i0.0$ | $0.0 + i0.0$ | $-0.1 + i0.0$ | $-0.1 + i0.1$ | $-0.2 + i0.1$ | $-0.3 + i0.2$ | $1.0 + i0.1$ | $-0.2 + i0.8$ |
| $\eta\Lambda$ | $0.0 + i0.0$ | $0.0 + i0.0$ | $0.0 + i0.0$ | $0.0 + i0.1$ | $0.0 + i0.1$ | $0.0 + i0.2$ | $0.7 + i0.0$ | $0.0 + i0.6$ |
| $K\Xi$ | $0.0 + i0.0$ | $0.0 + i0.0$ | $0.0 + i0.0$ | $0.0 + i0.0$ | $-0.1 + i0.1$ | $-0.1 + i0.1$ | $0.9 + i0.3$ | $-0.3 + i0.7$ |
| $\bar{K}^*N$ | $0.0 - i0.4$ | $0.0 - i0.5$ | $-0.1 - i0.5$ | $-0.1 - i0.5$ | $-0.1 - i0.6$ | $-0.2 - i0.6$ | $-0.4 + i1.3$ | $-1.0 - i0.6$ |
| $\omega\Lambda$ | $-0.5 + i0.3$ | $-0.5 + i0.3$ | $-0.6 + i0.3$ | $-0.6 + i0.3$ | $-0.6 + i0.2$ | $-0.6 + i0.1$ | $-0.2 + i1.1$ | $-1.2 - i0.0$ |
| $\rho\Sigma$ | $0.1 + i0.1$ | $0.1 + i0.1$ | $0.1 + i0.1$ | $0.1 + i0.0$ | $0.0 - i0.1$ | $-0.2 - i0.2$ | $-0.5 + i1.7$ | $-1.3 - i0.4$ |
| $\phi\Lambda$ | $0.7 - i0.4$ | $0.8 - i0.4$ | $0.9 - i0.4$ | $0.9 - i0.4$ | $0.9 - i0.4$ | $0.9 - i0.2$ | $0.5 - i1.6$ | $1.8 + i0.1$ |
| $K^*\Xi$ | $4.2 + i0.2$ | $4.3 + i0.2$ | $4.9 + i0.3$ | $4.7 + i0.3$ | $4.5 + i0.5$ | $4.3 + i1.1$ | $5.4 - i4.9$ | $6.6 + i4.1$ |

PB channels) we find an isoscalar pole at $1767 - i25$ MeV when PB and VB are not coupled (keeping $g_{\rm KR} = 0$). This pole couples strongly to the $K\Xi$ channel, as can be seen in Table X. By allowing the PB-VB systems to couple, we find that the coupling of this pole to the PB channels remains almost unchanged (see Table X). However it develops a very strong coupling to the $\rho\Sigma$ channel. The pole position is found to shift to lower energies while $g_{\rm KR}$ increases. It ends up at $1744 - i28$ MeV for $g_{\rm KR} = 6$. This value is still high as compared to the observed mass of the $\Lambda(1670)$ but we have shown that the inclusion of VB coupled channels improves the agreement.

The behavior of this pole can be seen in the $K\Xi$ amplitudes shown in Fig. 4, which hardly change with $g_{\rm KR}$, and

in the $\rho\Sigma$ amplitude in Fig. 5 which shows a clear peak near 1740 MeV for $g_{\rm KR} = 3$, 6 (dashed-dotted and solid curves).

#### *3. States with higher masses (in the range of 1800–2100 MeV):*

The main objective of the present work is to study the effect of the VB coupled channels on the low-lying resonances. In order to draw any concrete conclusion about higher mass resonances, we should take into account more complete VB $\rightarrow$ VB interactions as shown in Ref. [18]. However, within the present formalism, we can test if the widths of the resonances in 1800–2100 MeV region increase a lot by coupling the lower mass (PB) open channels.

In this energy region, we find three (spin degenerate) poles in the isospin 0 VB systems (with $g_{\rm KR} = 0$): $1795 - i0$ MeV, $1923 - i4$ MeV, and $2138 - i21$ MeV, quite in agreement with Ref. [3]. The little differences in the pole positions found in our work and Ref. [3] arise due to the differences in the calculations of the loops. First, we regularize the loops using a cutoff while the dimensional regularization scheme is used in Ref. [3]. We do not use the scheme of Ref. [3] since, as discussed in Sec. III A, it gives rise to an inappropriate behavior of the loops at energies much lower than the threshold. Second, to consider the fact that the vector mesons can sometimes possess considerably large widths, as is the case of $\rho$ and $K^*$, a convolution of the loops over the $\rho$ and $K^*$ widths was made for the related channels in Ref. [3] and, hence, the amplitudes and poles were obtained using the convoluted loops in the calculations. However, we restrict the calculation of the convoluted loops to the real energy axis because consideration of a varied mass for the vector mesons implies the presence of a band of (meson-baryon) thresholds instead of a fixed value, which sometimes makes it difficult to look for poles moving in the complex plane. This difficulty was also encountered by the authors of Ref. [3], although not in the case of systems with total isospin 0 and strangeness $-1$.

We would also like to remind the reader that although the VB interaction obtained from the $t$-channel exchange gives rise to spin independent amplitudes, the coupling of the PB and VB channels affects only the spin $1/2$ amplitudes. As a matter of course, in the present work we are only discussing the results obtained in the spin $1/2$ case.

To make the further discussion clearer, we will denote the (spin $1/2$) poles found in the VB systems at $1795 - i0$ MeV, $1923 - i4$ MeV, and $2138 - i21$ MeV as $P_i$, $P_{ii}$, and $P_{iii}$, respectively, since we cannot label them as $N^*$'s. This is so because a clear association of these poles to the known resonances cannot be made easily as the status of the known $N^*$ resonances in this energy region is very poor and a very little related information is available. Going back to the study of the poles, we find that the $P_i$, $P_{ii}$ poles move to higher energies as the coupling between the PB and VB systems increases (see Tables XI and XII).

For small values of $g_{\rm KR}$ (0–3), these poles are found to couple strongly to $\bar{K}^*N$ and $\rho\Sigma$, respectively. For $g_{\rm KR} = 4$, we find the coupling of the $P_i$ pole to the $\rho\Sigma$ and $\bar{K}^*N$ channel becomes comparable and the $P_{ii}$ pole becomes unphysical ($\rho\Sigma$ virtual state). For $g_{\rm KR} = 5$, we do not find any physical pole in 1800–2000 MeV but for $g_{\rm KR} = 6$ we find one physical pole at $1844 - i94$ MeV, which is listed in Table XI, although it cannot be connected to any of the two poles we started with. The couplings given in Table XI show that the pole found at $1844 - i94$ MeV can be interpreted as a $\rho\Sigma$ bound state.

The behavior of the poles $P_i$ and $P_{ii}$ can also be seen in the amplitudes shown in Fig. 5, most clearly in the $\rho\Sigma$ channel. The result corresponding to $g_{\rm KR} = 3$ (dashed-dotted line) shows three peaks; one for the $\Lambda(1670)$ and the other two related to the $P_i$ and $P_{ii}$ poles. Further, the solid line, which corresponds to the full PB-VB coupling, shows a peak near 1844 MeV.

The third pole found in the VB systems, in the 1800–2100 MeV region, denoted as $P_{iii}$, is found to couple strongly to $K^*\Xi$ (see Table XIII). This pole is found to shift to higher energies as the coupling between PB and VB channels increases, until $g_{\rm KR} = 6$ when we find a double pole structure with the pole positions being $2151 - i119$ MeV and $2160 - i73$ MeV. Both poles are found to couple strongly to the $K^*\Xi$ channel but the former one appears to couple to PB channels slightly more than the latter one.

To summarize, we started with three poles in the 1800–2100 MeV energy region in the VB systems uncoupled to PB: $1795 - i0$ MeV, $1923 - i4$ MeV, and $2138 - i21$ MeV and end up also with three poles in the PB-VB coupled systems: $1844 - i94$, $2151 - i119$ MeV, and $2160 - i73$ MeV but the nature of the latter set of poles is different as compared to the former ones.

An interesting finding of our work is that the width of the poles does not change a lot when they are allowed to couple to more open channels. Although such a notion exists that a pole would become moderately modified by taking into account those coupled channels, which consist of hadrons with the total mass much smaller than the mass of the resonance, it has not been explicitly verified earlier. Our results show that the general notion may not be very far from the reality.

### B. Isospin = 1

In the isospin 1 case, only one pole was found in the PB study of Ref. [30] at $1579 - i264$ MeV which was related to the $1/2^-$ $\Sigma(1620)$ resonance, although the width of the $\Sigma(1620)$ is $\leq 100$ MeV. Besides, this pole was found to be very sensitive to the subtraction constant parameters. Also, in the vector meson-baryon study of Ref. [10], two peaks were found in the amplitudes but no corresponding poles

were found in the complex plane. It was explained in Ref. [10] that finding poles was sometimes difficult due to the consideration of the widths of the vector mesons. We find that even without this consideration, i.e., without convoluting the loops, only one physical pole appears in isospin 1 VB systems, with its position being very close to the $\bar{K}^*N$ threshold. In view of the uncertain situation in the isospin 1 case, we do not try to adjust the cutoffs in our

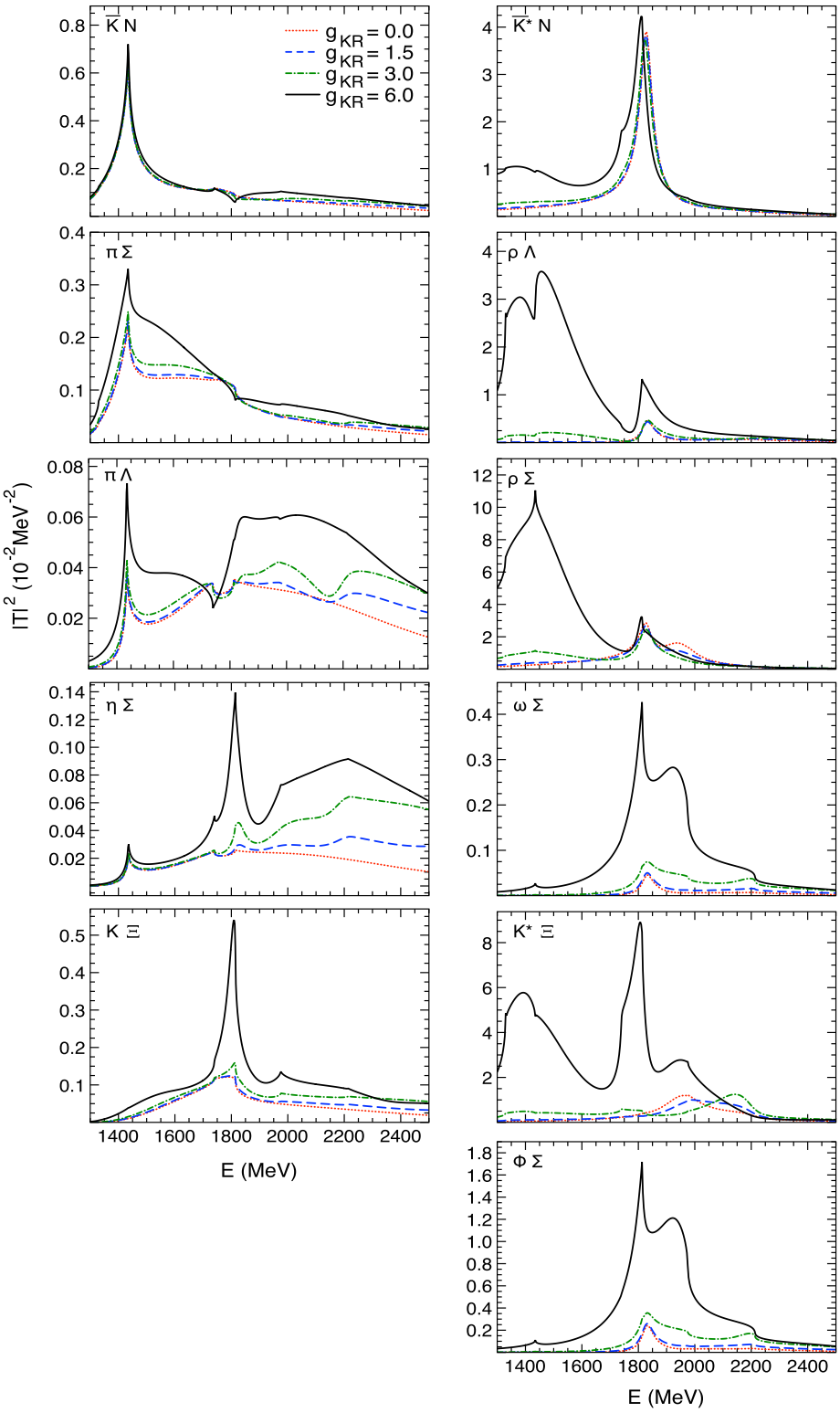


FIG. 6 (color online). Isospin 1 amplitudes of the PB and VB systems.

calculations to reproduce these poles. We, thus, keep the same cutoffs that we used in the isospin 0 case, which reproduce the results of the previous PB studies. We show the amplitudes obtained in this way for the uncoupled PB and VB systems in the isospin 1 configuration as dotted lines in Fig. 6. We find that these amplitudes are very similar to the ones obtained by calculating the loops with the dimensional regularization method as done in Refs. [3,10].

Corresponding to the amplitudes obtained with $g_{\rm KR} = 0$, we find a pole at $1479 - i285$ MeV in the PB systems and another at $1831 - i0$ in the VB systems. The pole obtained in the PB channels is found to couple mostly to $K\Xi$ and the one in the VB system couples mostly to $\bar{K}^*N$. We show the couplings of these poles to the related channels in Table XIV.

We now discuss the $T$ matrices calculated by coupling the PB and VB system with $g_{\rm KR} = 6$. The amplitudes found with $g_{\rm KR} = 6$ are shown by solid lines in Fig. 6. The calculation in the complex plane results in the finding of three poles at: $1426 - i143$ MeV, $1439 - i194$ MeV, and $2372 - i162$ MeV. These poles and their couplings to different channels are listed in Table XV. The poles at $1426 - i143$ MeV and $1439 - i194$ MeV couple mostly to $K^*\Xi$ and $\rho\Sigma$ channels, respectively. However these channels are closed for the decay of the corresponding resonances. The open channels which couple strongly to the pole at $1426 - i143$ MeV are $\bar{K}N$ and $\pi\Sigma$ and those which couple mostly to the $1439 - i194$ MeV state are $K\Xi$ and $\pi\Sigma$. These two poles could be associated with the $\Sigma(1480)$ resonance although very tentatively since it is reported to be much narrower ($\Gamma \sim 60$ MeV) [24,31]. It is important to notice that this resonance gets generated due to the PB-VB coupled channel effect and here we have used a simplified interaction for the VB interaction (since we focus here on the low-lying resonances). Thus, a more detailed VB interaction might improve the situation. It is also interesting to notice that a recent study of

TABLE XIV. $g^i$ couplings for the poles found in the uncoupled PB and VB systems in the isospin 1 configuration.

| $M_R - i\Gamma/2$ (MeV) → | $1479 - i285$ | $1831 - i0$ |
|---|---|---|
| Channels ↓ | Couplings ($g^i$) of the poles to the different channels | |
| $\bar{K}N$ | $0.4 - i1.1$ | $0.0 + i0.0$ |
| $\pi\Sigma$ | $1.4 - i1.6$ | $0.0 + i0.0$ |
| $\pi\Lambda$ | $-0.6 + i1.3$ | $0.0 + i0.0$ |
| $\eta\Sigma$ | $-0.5 + i1.2$ | $0.0 + i0.0$ |
| $K\Xi$ | $1.2 - i2.4$ | $0.0 + i0.0$ |
| $\bar{K}^*N$ | $0.0 + i0.0$ | $1.0 - i0.6$ |
| $\rho\Lambda$ | $0.0 + i0.0$ | $-0.7 + i0.4$ |
| $\rho\Sigma$ | $0.0 + i0.0$ | $-0.7 + i0.4$ |
| $\omega\Sigma$ | $0.0 + i0.0$ | $-0.4 + i0.2$ |
| $K^*\Xi$ | $0.0 + i0.0$ | $0.1 - i0.1$ |
| $\phi\Sigma$ | $0.0 + i0.0$ | $0.6 - i0.3$ |

TABLE XV. $g^i$ couplings for the poles found in the coupled PB-VB systems ($g_{\rm KR} = 6$) in the isospin 1 configuration.

| $M_R - i\Gamma/2$ (MeV) → | $1426 - i143$ | $1439 - i194$ | $2372 - i162$ |
|---|---|---|---|
| Channels ↓ | Couplings ($g^i$) of the poles to the different channels | | |
| $\bar{K}N$ | $-1.0 - i0.7$ | $0.7 + i0.3$ | $-0.1 + i0.0$ |
| $\pi\Sigma$ | $1.7 + i1.8$ | $1.2 + i1.3$ | $-0.5 + i0.2$ |
| $\pi\Lambda$ | $0.1 - i0.3$ | $-1.0 - i0.6$ | $0.3 - i0.2$ |
| $\eta\Sigma$ | $0.1 - i0.1$ | $-0.7 - i0.3$ | $0.3 - i0.2$ |
| $K\Xi$ | $0.7 + i0.8$ | $1.4 + i1.0$ | $-0.8 + i0.0$ |
| $\bar{K}^*N$ | $1.7 - i0.2$ | $2.6 - i0.1$ | $-0.1 - i0.1$ |
| $\rho\Lambda$ | $-5.6 + i0.5$ | $-5.8 + i1.1$ | $0.2 + i0.5$ |
| $\rho\Sigma$ | $4.5 - i0.2$ | $6.5 - i1.4$ | $-0.1 - i0.8$ |
| $\omega\Sigma$ | $-0.1 + i0.3$ | $0.2 + i0.1$ | $0.0 + i0.2$ |
| $K^*\Xi$ | $5.7 - i1.1$ | $5.0 - i1.1$ | $0.4 - i0.9$ |
| $\phi\Sigma$ | $0.2 - i0.5$ | $-0.3 - i0.2$ | $0.1 - i0.3$ |

the $K^- p \to \Lambda \pi^- \pi^+$ reaction shows a strong evidence of existence of a $\Sigma^*$ with $J^\pi = 1/2^-$ near 1400 MeV [32].

The pole at $2372 - i162$ MeV is found to couple mostly to the $K^*\Xi$ channel; however, we do not see a clear corresponding peak structure in the $K^*\Xi$ amplitude (shown in Fig. 6), which might be due to the presence of a negative interference of the pole with the background. A very little information is available about the $\Sigma$ states above 2 GeV region. Thus, for the moment, we do not relate our state with any known resonance.

## V. SUMMARY

The work discussed in this manuscript can be summarized as follows:

(1) In order to study dynamically generated resonances in the PB-VB coupled systems, we find that the cutoff method together with a Gaussian form factor is more suitable to calculate the loops, which satisfy unitarity conditions, as well as the dispersion relations.

(2) Coupling VB to the PB systems with strangeness $-1$ and isospin 0 reveals large coupling of the low-lying $\Lambda$ resonances to the closed VB channels, although the pole positions and the couplings of these resonances to the PB channels remain almost unaltered. It is important to mention here that the large coupling of the low-lying $\Lambda$'s to the VB channels found in our work do not imply the presence of a large fraction of VB component in the wave function of these resonances since the large mass difference between the two would suppress it. Therefore, the interpretation of the low-lying $\Lambda$'s as PB molecular states does not change. However, our findings could have some implications on, for example, the photoproduction of the $\Lambda$ resonances where the production mechanism proceeding through exchange of a vector meson could become important [33]. This should be verified in future.

(3) The isoscalar states with higher masses, which have earlier been found to get generated in VB systems, do not get much wider by coupling the open PB channels.

(4) In the isospin 1 case, a double pole structure is found near 1430 MeV and we tentatively relate this to the $\Sigma(1480)$ [24,31].

## ACKNOWLEDGMENTS

This work is partly supported by the Grant-in-Aid for Scientific Research on Priority Areas titled "Elucidation of New Hadrons with a Variety of Flavors" (E01: 21105006 for K. P. K. and A. H.) and (22105510 for H. N.) and the authors acknowledge the same. A. M. T. is thankful to the support from the Grant-in-Aid for the Global COE Program "The Next Generation of Physics, Spun from Universality and Emergence" from the Ministry of Education, Culture, Sports, Science and Technology (MEXT) of Japan.

[1] N. Kaiser, P. B. Siegel, and W. Weise, Nucl. Phys. **A594**, 325 (1995).
[2] N. Kaiser, P. B. Siegel, and W. Weise, Phys. Lett. B **362**, 23 (1995).
[3] E. Oset and A. Ramos, Nucl. Phys. **A635**, 99 (1998).
[4] T. Inoue, E. Oset, and M. J. Vicente Vacas, Phys. Rev. C **65**, 035204 (2002).
[5] D. Gamermann, C. Garcia-Recio, J. Nieves, and L. L. Salcedo, Phys. Rev. D **84**, 056017 (2011).
[6] Y. Yamaguchi, S. Ohkoda, S. Yasui, and A. Hosaka, Phys. Rev. D **84**, 014032 (2011).
[7] T. Hyodo, S. I. Nam, D. Jido, and A. Hosaka, Phys. Rev. C **68**, 018201 (2003).
[8] C. E. Jimenez-Tejero, A. Ramos, and I. Vidana, Phys. Rev. C **80**, 055206 (2009).
[9] J. A. Oller and U. G. Meissner, Phys. Lett. B **500**, 263 (2001).
[10] E. Oset and A. Ramos, Eur. Phys. J. A **44**, 445 (2010).
[11] D. Gamermann, C. Garcia-Recio, J. Nieves, L. L. Salcedo, and L. Tolos, Phys. Rev. D **81**, 094016 (2010).
[12] M. Doring, C. Hanhart, F. Huang, S. Krewald, and U. G. Meissner, Nucl. Phys. **A829**, 170 (2009).
[13] A. Martinez Torres and D. Jido, Phys. Rev. C **82**, 038202 (2010); A. Martinez Torres, K. P. Khemchandani, and E. Oset, Phys. Rev. C **79**, 065207 (2009).
[14] K. P. Khemchandani, A. Martinez Torres, and E. Oset, AIP Conf. Proc. **1322**, 379 (2010); K. P. Khemchandani, A. Martinez Torres, and E. Oset, Eur. Phys. J. A **37**, 233 (2008).
[15] S. Sarkar, B.-X. Sun, E. Oset, and M. J. Vicente Vacas, Eur. Phys. J. A **44**, 431 (2010).
[16] D. Jido, J. A. Oller, E. Oset, A. Ramos, and U. G. Meissner, Nucl. Phys. **A725**, 181 (2003).
[17] T. Hyodo and D. Jido, arXiv:1104.4474.
[18] K. P. Khemchandani, H. Kaneko, H. Nagahiro, and A. Hosaka, Phys. Rev. D **83**, 114041 (2011).
[19] E. Oset, E. J. Garzon, J. J. Xie, P. Gonzalez, A. Ramos, and A. M. Torres, arXiv:1103.0807.
[20] N. M. Kroll and M. A. Ruderman, Phys. Rev. **93**, 233 (1954).
[21] M. Bando, T. Kugo, and K. Yamawaki, Nucl. Phys. **B259**, 493 (1985).
[22] T. Yamanishi, Phys. Rev. D **76**, 014006 (2007).
[23] J. A. Oller, Eur. Phys. J. A **28**, 63 (2006).
[24] K. Nakamura *et al.* (Particle Data Group), J. Phys. G **37**, 075021 (2010).

[25] A. Martinez Torres, K. P. Khemchandani, and E. Oset, Phys. Rev. C **77**, 042203 (2008).
[26] P. Gao, B. S. Zou, and A. Sibirtsev, Nucl. Phys. **A867**, 41 (2011).
[27] J. A. Oller and E. Oset, Nucl. Phys. **A620**, 438 (1997).
[28] T. Hyodo, D. Jido, and A. Hosaka, Phys. Rev. C **78**, 025203 (2008).
[29] J.-J. Wu and B. S. Zou, arXiv:1011.5743.
[30] E. Oset, A. Ramos, and C. Bennhold, Phys. Lett. B **527**, 99 (2002).
[31] I. Zychor, V. Koptev, M. Buscher, A. Dzyuba, I. Keshelashvili, V. Kleber, H. R. Koch, and S. Krewald *et al.*, Phys. Rev. Lett. **96**, 012002 (2006).
[32] J.-J. Wu, S. Dulat, and B. S. Zou, Phys. Rev. C **81**, 045210 (2010); Phys. Rev. D **80**, 017503 (2009).
[33] S.-i. Nam, J.-H. Park, A. Hosaka, and H.-C. Kim, arXiv:0806.4029.